Phonon–spin scattering and magnetic heat transport in the quasi-one-dimensional spin-1/2 antiferromagnetic chain compound CuSb_{2}O_{6}

N. Prasai, A. Rebello, A. B. Christian, J. J. Neumeier, and J. L. Cohn

Phys. Rev. B **91**, 054403 — Published 11 February 2015

DOI: 10.1103/PhysRevB.91.054403

Phonon-spin scattering and magnetic heat transport in the quasi-one-dimensional spin-1/2 antiferromagnetic chain compound, $CuSb_2O_6$

N. Prasai,[1] A. Rebello,[1] A. B. Christian,[2] J. J. Neumeier,[2] and J. L. Cohn[1]

[1] *Department of Physics, University of Miami, Coral Gables, FL 33124*
[2] *Department of Physics, Montana State University, Bozeman, Montana 59717*

(Dated: January 26, 2015)

We report measurements of thermal conductivity (κ) on single crystals of the quasi-one-dimensional spin-1/2 anitferromagnetic (AF) chain compound $CuSb_2O_6$ and its non-magnetic analog $ZnSb_2O_6$ in the temperature range 5K $\leq$ T $\leq$ 300K. A substantially lower κ for $CuSb_2O_6$ compared to that of $ZnSb_2O_6$ has its origin in resonant phonon-spin scattering involving excitation of a two-level system (energy scale $\sim$ 100 K) associated with the onset of local spin order at $T \leq 150$ K. Anisotropy in κ for the $CuSb_2O_6$ also emerges at $T \leq 150$K and might be associated with a magnetic contribution to heat transport. A magnetic mean-free-path comparable to that of other spin-1/2 linear-chain compounds (~ 0.3 μm) is implied.

PACS numbers: 66.70.-f, 75.10.Jm,65.40.-b, 61.05.cp

I. INTRODUCTION

Low-dimensional quantum spin systems have attracted considerable interest in recent years for their role in the development of many-body theory[1] and for experimental observations of substantial heat conduction associated with spin excitations.[2,3] To date, most thermal conductivity investigations have focused on quasi-one-dimensional (q1D) spin-1/2 chain systems with exchange energies much greater than the Debye temperature ($J \gg \Theta$),[2,3] where spin heat conduction is often distinguishable from that of the lattice by their different temperature scales. The situation is potentially more complex when spin and phonon energy scales are comparable since interactions between the two subsystems become more significant and can lead to dimerization of magnetic ions (spin-Peierls transition). At least one system having $J \sim \Theta$ for which a spin thermal conductivity has been inferred from κ measurements,[4] has a spin mean-free-path (l_{mag}) comparable to that in large J systems, suggesting similar relaxation characteristics.

$CuSb_2O_6$ has a monoclinically-distorted trirutile structure[5] below 380 K with nearly undistorted CuO_6 octahedra. In spite of its two-dimensional layered structure of CuO plaquettes, its magnetism is quasi-one-dimensional, with magnetic susceptibility well-described by a nearest-neighbor-only, spin-1/2 Heisenberg antiferromagnetic (AF) chain model and exchange coupling strength $J \approx 90 - 100$ K. Long-range AF order is established below $T_N \approx 8.7$ K.[6–14] Electronic structure calculations[15] reveal that the unusual quasi-1D magnetic ground state is driven by orbital ordering, attributed to the presence of competing in- and out-of plaquette orbitals and strong electronic correlations.

The strongest exchange interactions are expected to be along the [110] (at $z = 0$) and [$\bar{1}$10] (at $z = 1/2$) directions where the angle of the Cu-O-O-Cu bonds of adjacent CuO_6 octahedra are close to 180°. Interchain exchange is much weaker due to a larger Cu-O bondlength and 160° Cu-O-Cu bond angle. Though some discrepancy exists in the literature regarding the appropriate magnetic structure in the ordered state, single-crystal neutron scattering studies[9,13] and recent magnetic susceptibility and specific heat studies of the related compounds[16] $CoSb_2O_6$ and $NiTa_2O_6$, indicate magnetic moments aligned nearly parallel to [010], in ferromagnetic lines along [010] and alternating antiparallel lines along [100] [magnetic wave vector $(\pi/a, 0, \pi/c)$].

Recent heat capacity and thermal expansion studies[14] of $CuSb_2O_6$ and its non-magnetic analog $ZnSb_2O_6$ reveal short-range q1D AF order appearing in $CuSb_2O_6$ at $T \geq 120$ K and unusual character of a spin-Peierls-like transition at T_N and the opening of an energy gap[13,14] with energy scale $\sim$ 17.5 K. Here we report a systematic study of thermal conductivity (κ) in single crystals of these compounds. We find that κ for $CuSb_2O_6$ is substantially suppressed compared to that of $ZnSb_2O_6$ over a broad temperature range as a consequence of phonon-spin resonant scattering. This scattering is associated with the onset of the short-range q1D AF correlations below 150 K. This resonant scattering is modeled as a two-level system with energy splitting $\sim$ 100 K, consistent with a similar analysis of the magnetic contribution to the specific heat and thermal expansion. A substantial anisotropy of κ in $CuSb_2O_6$ also develops below 150 K and might be associated with magnetic heat conduction within the plane of the spin chains. The inferred low-T magnetic mean-free-path, $l_{mag} \sim 0.3\mu$m, is comparable to that found for other spin-1/2 chain systems.

II. EXPERIMENT

Single-crystal growth of monoclinic $CuSb_2O_6$ and tetragonal $ZnSb_2O_6$ using a chemical vapor transport method is described in detail elsewhere.[10,14] X-ray diffraction was used to determine the orientation and crystallographic structure of the crystals. Lattice param-

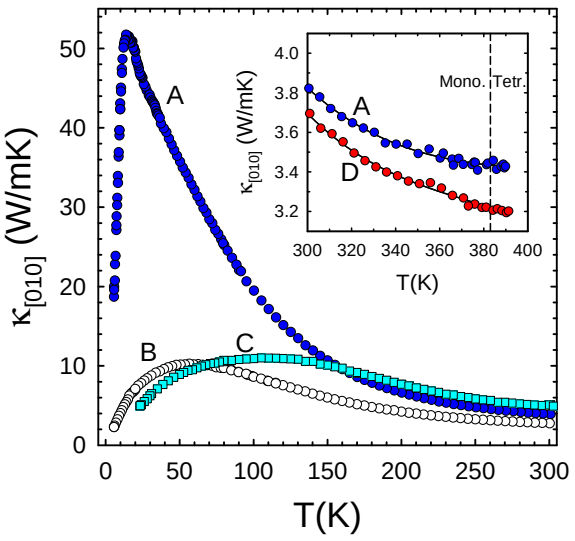

FIG. 1. (Color online) Thermal conductivity *vs.* temperature along the [010] direction for three $CuSb_2O_6$ crystals. Substantially reduced low-T magnitudes are observed for bicrystals (B and C) as compared to the monodomain crystal (A). Inset: high-T data through the tetragonal-monoclinic structural transition at 383 K (dashed line) for two crystals.

eters determined from high-angle extrapolation[17] of reflections from various lattice planes were a=4.637(9) Å, b=4.638(6) Å , c=9.304(2) Å and β=91.1(2)° for $CuSb_2O_6$, and a=4.653(3) Å, c=9.280(2) Å for $ZnSb_2O_6$, in good agreement with prior reports for these compounds.[10,18] The quality of the crystals was evident in rocking-curve widths (FWHM) $\Delta\omega \lesssim 0.06°$ for their (006) reflections. For for $CuSb_2O_6$ thermal conductivity was measured with heat flow along the principle crystallographic axes and also along the spin chains, [110]. The short dimension of the $ZnSb_2O_6$ crystals along [001] precluded measurements in that direction; data along [100] are reported here. A standard steady-state method was employed with temperature gradient produced by a chip heater and monitored by a 25-μm diameter chromel-constantan differential thermocouple, both attached with stycast epoxy.

III. DATA AND DISCUSSION

A. Twinning and Bicrystallinity

Characterizing individual crystals with x-ray diffraction (XRD) proved essential to determining intrinsic thermal conductivities of these compounds because of the potential for bicrystallinity. The presence of two crystalline domains was not readily apparent upon visual inspection and in some cases was not detected in Laue images. However, bicrystalline specimens had dramatically suppressed thermal conductivities (Fig. 1), evidently due to substantial phonon scattering at domain boundaries. Such crystals were excluded from subsequent study. Twinning, associated with the tetragonal to monoclinic transition (383 K), was evidenced in triple-split (013)-plane reflections in XRD,[10] corresponding to (013), (103), and ($\bar{1}$03), respectively. Two principal twin variants are implied: (1) 180° rotations of the b-c plane about the a axis [Fig. 2 (a)] and (2) 90° rotations of the a-b plane about the c axis (i.e. a swapping of a and b orientations). Azimuthal (ϕ) scans of the (039) and (309) reflections [Fig. 2 (b)] demonstrate that the [100] and [010] directions remain distinguishable and thus twins of variant (2) are in the minority.

To investigate the possible role of these twins on the heat transport, κ for two specimens was measured in a separate high-T vacuum probe to T = 390 K (Fig 1, inset), i.e. above the structural transition where the structural twins are known to disappear.[10] These data show no abrupt increase in κ at the phase transition temperature as would be expected if twin boundaries were strong phonon scatters. We thus conclude that such growth twins have little influence on the heat transport of the Cu compound near room temperature and above.

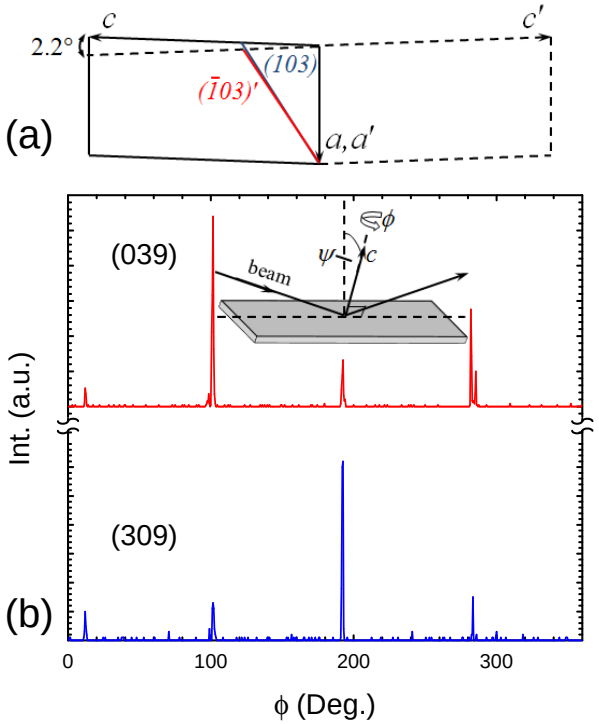

FIG. 2. (Color online) (a) scheme of twin variant (1) inferred from XRD for $CuSb_2O_6$ crystals. (b) ϕ scans at $\psi = 33.5° \simeq \tan^{-1}(c/3a)$ for the (039) and (309) reflections. Inset shows the geometry of the XRD scans for crystals oriented with their c axes along the thinnest direction.

B. Results for $\kappa(T)$

Figure 3 shows $\kappa(T)$ for $CuSb_2O_6$ and $ZnSb_2O_6$ crystals with heat flow along various crystallographic directions. Most striking is the substantially larger κ for nonmagnetic $ZnSb_2O_6$ throughout most of the temperature range, which, as established in the preceding sections, cannot be attributed to twinning or poor crystallinity of the Cu compound. The maximum at $T = 30$ K is typical of crystalline insulators[19] near $\Theta/20$ (Θ is the Debye temperature), occurring as the dominant phonon scattering changes from anharmonic phonon-phonon at high temperatures to defect and boundary scattering at low temperatures. Both compounds have similar Debye temperatures[14] and thus we should expect this maximum at a similar temperature for the Cu compound. The implication is that substantial additional scattering of phonons is operative in $CuSb_2O_6$. κ becomes anisotropic for $CuSb_2O_6$ at $T \lesssim 150$K. Along [100] and [001] $\kappa(T)$ exhibits a dip-like feature at $40-50$ K. Hints of this feature are also evident along [010] and [110], but the magnitude of κ along these directions is significantly higher. The sensitivity of κ within the a-b plane to mis-alignment of the crystallographic axes is demonstrated by the pairs of data sets (designated by arrows in Fig. 3), for nominally [110] and [100] orientations. For these orientations, the curves with lower magnitude below 20 K correspond to crystals that were mis-aligned out of the a-b plane by 5° or more, and thus had a component of the heat flow oriented along [001]. All other crystals were oriented to within 1°.

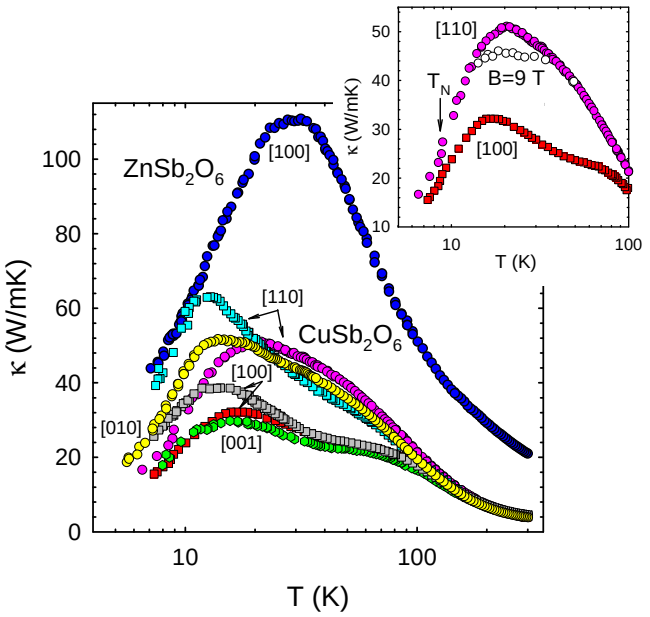

FIG. 3. (color online) Thermal conductivity of $CuSb_2O_6$ and $ZnSb_2O_6$ single crystals with heat flow along the crystallographic directions indicated. Inset: zero-field and $B = 9$T data (open circles) for one of the $CuSb_2O_6$ specimens along [110]. A slight downturn in κ below T_N is evident (arrow) in the data for two specimens.

The magnetic field dependence of κ was modest in magnitude; data for a specimen measured along [110] with a 9-T field oriented along the heat flow is shown in the inset of Fig. 3. A suppression of κ by $\sim 10\%$ was observed near the zero-field maximum. Also evident in this figure is a slight downturn in κ below T_N for this specimen and for that measured along [100].

C. Phonon-spin resonant scattering

First consider the source of additional phonon scattering that underlies the much smaller $\kappa(T)$ found for $CuSb_2O_6$ relative to that of $ZnSb_2O_6$ over most of the temperature range. This scattering is responsible for the dip in $\kappa(T)$ curves noted above. Such features are the signature of resonant scattering in which heat-carrying phonons are strongly damped over a restricted frequency range. The dominant phonons responsible for κ have energies $\sim 3.8k_BT$, thus we anticipate a resonant interaction for phonons with energies $\sim 13-16$ meV.

Any suppression of κ attributed to resonant phonon-spin scattering must be relatively isotropic given that it is evident for heat flow both within and perpendicular to the plane of the spin chains. This suggests an interaction between phonons and *localized* spin states rather than dispersive states with momenta confined to the a-b planes. A mechanism like this was introduced[21] to describe resonant phonon-spin scattering in the two-dimensional spin-dimer system $SrCu_2(BO_3)_2$: a phonon excites the spin system and under deexcitation a phonon emitted with the same energy is uncorrelated in its direction with the first (the initial and final spin states are the same).

Further insight into the resonant scattering mechanism is found in specific heat and thermal expansion studies[14] of $ZnSb_2O_6$ and $CuSb_2O_6$. Figure 4 shows $\kappa(T)$ data along the [100], [001], and [110] directions for $CuSb_2O_6$ on an expanded linear scale for $T \leq 175$ K along with the magnetic specific heat, $C_{mag} = C_p(\mathrm{Cu}) - C_p(\mathrm{Zn})$, and the difference in the a- and c-axis linear thermal expansion coefficients for Cu and Zn compounds, $\Delta\mu_i = \mu_i(\mathrm{Cu}) - \mu_i(\mathrm{Zn})$ ($i = a,\ c$). Note that $\mu_a \approx \mu_b$ throughout this temperature regime, and since $\mu_c(\mathrm{Cu})$ is negative we plot $|\Delta\mu_c|$. Two features are noteworthy. The rise in C_{mag} and the $\Delta\mu_i$ below $T \simeq 150$ K, which signal the onset of spin correlations and associated anharmonicity, respectively, in the Cu compound,[14] coincide with the onset of anisotropy in $\kappa(T)$. The maxima in the magnitudes of C_{mag} and the $\Delta\mu_i$ at $T \simeq 40-50$ K coincide with the "dip" in $\kappa(T)$ noted above for both the [100] and [001] directions.

Unlike the case in strongly-coupled spin-Peierls systems (e.g.,[22] $CuGeO_3$) where the Néel transition involves dimerization of spins and substantial lattice distortions, the specific heat and thermal expansion for

$CuSb_2O_6$ indicate a gradual loss of spin entropy[14] associated with *local* 1D spin ordering and lattice modifications beginning well above $T_N = 8.7$ K. By implication, the resonance-like phonon scattering evidenced in $\kappa(T)$ involves phonon-induced excitations of the locally ordered spin chains.

The maxima in C_{mag} and the $\Delta\mu_i$ are reminiscent of Schottky anomalies for two-level systems, though this is an oversimplification since the loss of spin entropy[14] from 120 K to T_N is $\sim 60\%$ of $R\ln 2$. In the simplest case (Grüneisen scaling), $\Delta\mu \propto C_{mag}$:[23]

$$\Delta C_{mag} = k_B \left(\frac{\varepsilon}{T}\right)^2 \frac{e^{-\varepsilon/T}}{\left(1+e^{-\varepsilon/T}\right)^2},$$
$$\Delta\mu_i = \frac{1}{V_{fu}} \frac{\partial \ln \varepsilon}{\partial p_i} \Delta C_{mag},$$

where ε is the energy splitting, V_{fu} is the formula unit volume, and p_i the uniaxial pressure. The $\Delta\mu_i$ and C_{mag} can have different T dependencies when the pressure derivative depends on T or when there are more than two levels each with independent pressure derivatives. Allowing for different effective values for ε, the dashed curves in Fig. 4 give reasonable approximations to experiment and correspond to the above expressions (with the addition of a small constant terms, 0.2 J/mol K^2 for C_{mag} and 3×10^{-7} K^{-1} for the $\Delta\mu_i$) using $\varepsilon = 85$ K for C_{mag} and $\partial \ln\varepsilon/\partial p_i = 4.35\times10^{-10}$ Pa^{-1} (1.52×10^{-10} Pa^{-1}),

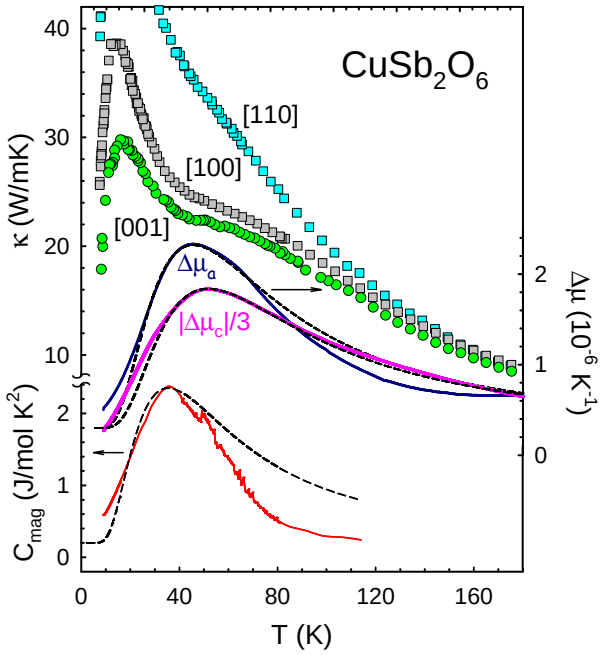

FIG. 4. (color online) Thermal conductivity for $CuSb_2O_6$ along the [100], [001] and [110] directions (top left ordinate), difference in linear thermal expansion coefficients of $CuSb_2O_6$ and $ZnSb_2O_6$ (right ordinate) and magnetic specific heat (lower left ordinate) from Ref. 14. Dashed curves are fits to the Schottky expression (see text).

$\varepsilon = 109$ K (124 K) for the a-axis (c-axis) expansion coefficients. As we discuss in the next section, this energy scale $\varepsilon \sim 100$ K also describes the resonant scattering in κ.

A clear physical picture of the relevant lattice/spin excitations and their scattering of heat-carrying phonons remains to be established. Inelastic neutron scattering studies[13] of $CuSb_2O_6$ identified a strong resonance feature at energy $\sim$ 13 meV in the magnetic excitation spectrum for momentum transfer $q = 3\pi/4a$ along the [100] direction. This is close to where the free spinon dispersion has a maximum[20] at $(\pi/2)J$. This resonance is observed well above T_N and grows in intensity with decreasing T, and is thus likely related to the development of short range magnetic order. Based on its unusual intensity distribution, the resonance was proposed[13] to couple with B_{1g} optical phonons which involve rotations of the CuO_6 octahedra about the [001] direction and thereby modulate the Cu-O-O-Cu bond angle and superexchange interaction along [110]. However, the B_{1g} mode is strongly dispersing in the rutile structure[24] and is expected at energies > 20 meV at the momentum corresponding to the resonance. This mode involves only oxygen motions, and thus it is unlikely that in the trirutile structure of $CuSb_2O_6$ it would be found at a much lower energy compatible with that of the resonance.

In Ref. 14 it was proposed that the short-range magnetic order at $T \geq T_N$ reflects the formation of *local* spin-Peierls ordered domains (e.g., dimerized chain fragments). Such a scenario has the potential to reconcile the absence of typical spin-Peierls anomalies in the specific heat and thermal expansion at T_N and the appearance of a gap at $T \leq T_N$. This raises the possibility that the $\sim$ 100 K energy scale evidenced in the thermodynamic properties and thermal transport, comparable to J, is connected with singlet-triplet excitations. Further theoretical and experimental work are required to address this speculation.

D. Modeling the $\kappa(T)$ Data

Calloway model[19] fitting to the data was employed to quantify the additional phonon scattering that operates in the magnetic Cu compound. $\kappa(T)$ was computed as:

$$\kappa_L = \frac{k_B}{2\pi^2 v_{ph}} \left(\frac{k_B T}{\hbar}\right)^3 \int_0^{\Theta/T} \frac{x^4 e^x}{(e^x-1)^2} \tau(\omega, T) dx,$$

where $x = \hbar\omega/k_B T$, ω is the phonon angular frequency, and $\tau(\omega, T)$ is the phonon relaxation time. The Debye temperature is computed from the average phonon velocity (v_{ph}) as $\Theta = (\hbar v_{ph}/k_B)(6\pi^2 n)^{1/3}$, where n is the atom density.

We first fitted the $\kappa(T)$ data for $ZnSb_2O_6$ by incorporating phonon scattering terms representing boundaries,

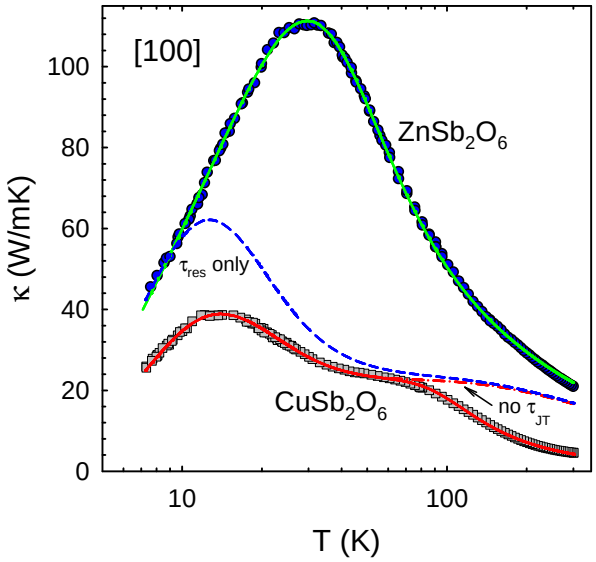

FIG. 5. (color online) Model fitting to $\kappa_{[100]}$ data for $ZnSb_2O_6$ and $CuSb_2O_6$. Parameter values in common to both specimens (see text) for the best fits (solid curves) were: v_{ph} = 4.8 km/s, $B = 1.05 \times 10^{-18}$ sK^{-1}, $b = 6.5$. The point-defect terms were $A = 2.46\ (2.19) \times 10^{-43}$ s^3 for $ZnSb_2O_6$ ($CuSb_2O_6$). Additional scattering terms for $CuSb_2O_6$ were: $C = 5.55\times10^{-18}$ s^2, $R = 2.49\times10^{-34}$ s^3, $D = 2.22\times10^{-41}$ s^3. Also shown are curves for the Cu compound excluding all but the resonant scattering term (dashed curve) and with all terms except the Jahn-Teller term (dash-dotted curve).

point defects, and Umklapp processes, respectively:

$$\tau(\omega,T)^{-1} = \frac{v_{ph}}{L_b} + A\omega^4 + B\omega^2 T \exp\left(-\frac{\Theta}{bT}\right),$$

where L_b is taken as the minimum sample dimension, and A, B, and b are fitting parameters. The phonon velocity was taken as v_{ph} = 4.8 km/s, an average of the rutile sound velocities.[24] The results of the fitting and parameter values are included in Fig. 5 and its caption.

Fitting to the $CuSb_2O_6$ [100] (or [001]) data employed the same values for v_{ph}, B, and b as for the $ZnSb_2O_6$ fitting and included three additional scattering terms. At the lowest temperatures a sheet-like fault scattering term, $C\omega^2$, was introduced to account for the much lower magnitude of κ in the Cu compound – this term is attributed to scattering from twin boundaries. Resonant scattering from the two-level magnetic system was represented as,[25–27]

$$\tau_{res}(\omega,T)^{-1} = R\frac{\omega^4}{(\omega^2-\omega_0^2)^2}F(T),$$

where R is the scattering strength, ω_0 is the resonance frequency, and $F(T)$ is a factor that accounts for thermal occupancies of the two states. Two-level systems that exist only at the interface between ordered and "not yet ordered" regions, i.e. domains of high strain, would suggest $F(T) = n_0(1-n_0)$, where $n_0 = [1+\exp(-\hbar\omega_0/k_BT)]^{-1}$ is the fraction of two-level systems in the ground state. The best fit using this form for $F(T)$ (Fig. 5) yields a resonance energy, $E_0 = \hbar\omega_0/k_B$ = 67 K, comparable to but somewhat smaller than the two-level energy splittings found from the specific heat and thermal expansion. If $F(T)$ defines a narrower range in T then the fitted value for E_0 increases. For example, taking $F(T)$ to be the full Schottky function, $(E_0/T)^2 n_0(1-n_0)$, yields a best fit of comparable quality with E_0 = 105 K. Thus the resonance energy inferred from the fitting is in reasonable accord with the two-level energy splitting. To distinguish the influence of these additional scattering terms, Fig. 5 also shows the computed $\kappa(T)$ including only the resonant scattering term (dashed line) and both the resonant and sheet-like fault scattering terms (dash-dotted).

A third term was introduced to account for additional scattering, evident above 100 K in Fig. 5, that we attribute to the dynamic Jahn-Teller effect, a feature of the tetragonal phase of the Cu compound at $T > 383$ K that freezes out gradually at temperatures below the tetragonal-monoclinic transition. It involves thermal excitation of different orientations of the elongated Cu-O bonds of the two inequivalent CuO_6 octahedra within the unit cell,[5] and is reflected in the T dependence of the monoclinic β angle which serves as an order parameter for the transition and becomes T independent at $T \leq 100$ K.[11] Such dynamic local distortions of the octahedra are anticipated to behave as point defect scatterers of heat-carrying phonons with a thermally activated scattering rate determined by the characteristic optical phonon energy scale. A term $\tau_{JT}^{-1} = D\omega^4\exp(-490/T)$ described the additional scattering well (Fig. 5). The phonon energy, 490 K$\simeq$ 42 meV, agrees with electron-spin-resonance studies[11] which indicate a phonon at 44 meV responsible for spin-lattice relaxation in the tetragonal phase.

E. Magnetic heat transport?

We now address the anisotropy in κ that develops in $CuSb_2O_6$ at $T \leq 150$ K. Given that the spin-chain direction alternates (moving along the [001] direction) between [110] and [$\bar{1}$10], magnetic heat transport (κ_{mag}) is anticipated within the a-b planes but not along c. The surprising result is that $\kappa_{[100]}$ is much smaller than $\kappa_{[010]}$ and $\kappa_{[110]}$ in the range 10 K$\leq T \leq$ 150 K. The convergence of $\kappa_{[100]}$ and $\kappa_{[010]}$ at $T < 10$ K indicates isotropy of the a-b plane lattice thermal conductivity as would be expected based on the crystal structure. One possibility is that the resonant phonon scattering is anisotropic within the a-b plane, i.e. weaker for transport along the [010] and [110] directions, though this seems less plausible given that $\kappa_{[100]}(T)$ and $\kappa_{[001]}(T)$ are indistinguishable for $T \geq 30$ K as are the [100] and [010] thermal expansion coefficients.[14] An alternative hypothesis is that the enhanced κ along [010] and [110] is associated with a κ_{mag} and this contribution is preferentially suppressed

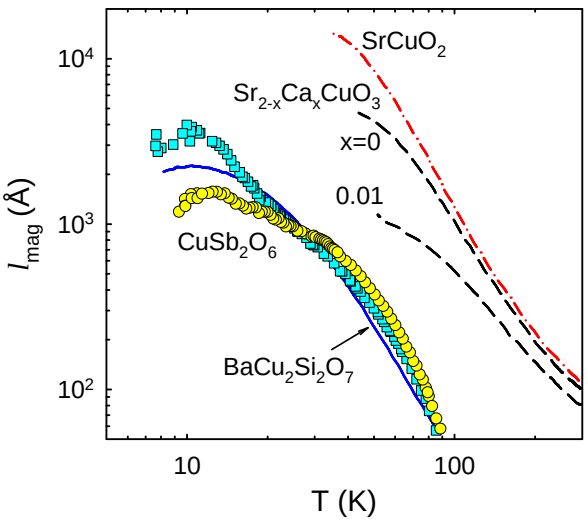

FIG. 6. (color online) Magnetic mean-free-path for [110] and [010] directions of $CuSb_2O_6$ (symbols) computed by subtracting $\kappa_{[100]}(T)$ to determine κ_{mag} (see text). Also shown for comparison are results from other spin-1/2 chain compounds: $BaCu_2Si_2O_7$ (Ref. 4), $SrCuO_2$ (Ref. 28), and $Sr_{2-x}Ca_xCuO_3$ (Ref. 29)

along [100]. This might have its origin in the nature of the local 1D magnetic ordering (e.g. chain fragments) or its interplay with the twinning [Fig. 2 (a)]. Measurements of κ in detwinned crystals might offer a means of testing this hypothesis, but previous efforts at detwinning were not successful.[10]

To examine the plausibility of our hypothesis about magnetic heat transport we estimated κ_{mag} for the [110] and [010] directions by subtracting, from the corresponding $\kappa(T)$ curves, the data for $\kappa_{[100]}$ (using $\kappa_{[001]}$ for this subtraction would overestimate κ_{mag} at low T since our data implies a larger a-b plane lattice thermal conductivity). We then computed a mean-free-path, using,[29] $l_{mag} = (3\hbar/\pi N_s k_B^2 T)\kappa_{mag}$, where $N_s = 2/(\sqrt{2}ac)$ is the number of chains per unit area appropriate to $CuSb_2O_6$. Figure 6 shows the resulting $l_{mag}(T)$ for the present specimens and for comparison, those of other Q1D $s = 1/2$ chain compounds $BaCu_2Si_2O_7$,[4] $SrCuO_2$,[28] and $Sr_{2-x}Ca_xCuO_3$,[29] computed similarly. We see that l_{mag} for $CuSb_2O_6$ is similar in its T dependence and low-T magnitude ($\sim 0.1 - 0.3$ μm) to that of $BaCu_2Si_2O_7$, suggesting a universal behavior (when suitably scaled by J) for $s = 1/2$ chain systems as noted previously.[4]

Regarding the magnetic transition, the [110] and [010] specimens do not exhibit a downturn in κ just below T_N seen for the mis-aligned specimens (inset, Fig. 3). This suggests that this feature is associated with the lattice thermal conductivity and that the opening of an energy gap[13,14] below T_N does not have a strong effect on the magnetic heat transport.

IV. CONCLUSIONS

In summary, thermal conductivity studies of single-crystal $CuSb_2O_6$ and $ZnSb_2O_6$ reveal strong phonon-spin resonant scattering in $CuSb_2O_6$ associated with the onset of short-range q1D AF order at $T \leq 150$ K. Anisotropy of κ within the plane of the spin chains, developing at $T \leq 150$ K, indicates either anisotropy of the resonant scattering or the onset of a magnetic contribution to heat transport that is preferentially suppressed along the [100] direction (possibly related to the twinning). The inferred magnetic contribution to heat conduction is consistent with that found in other low-dimensional spin systems. The scattering resonance energy ~ 100 K is consistent with the energy splitting of a two-level Schottky model that describes the magnetic contribution to the specific heat and linear thermal expansion coefficients. The nature of the excited state, likely involving spin and lattice perturbations, remains to be determined.

ACKNOWLEDGMENTS

This material is based upon work supported by the U.S. Department of Energy (DOE)/Basic Energy Sciences (BES) Grant No. DE-FG02-12ER46888 (Univ. Miami) and National Science Foundation under grant DMR-0907036 (Mont. St. Univ.).

[1] X. Zotos and P. Prelovśek, in *Strong Interactions in Low Dimensions*, D. Baeriswyl and L. Degiorgi (eds.), Kluwer Academic Publishers, Dordrecht (2004), p. 347.
[2] C. Hess, Eur. Phys. J. Special Topics **151**, 73 (2007).
[3] A. V. Sologubenko, T. Lorenz, H. R. Ott, and A. Freimuth, J. Low T. Phys. **47**, 387 (2007).
[4] A. V. Sologubenko, H. R. Ott, G. Dhalenne, and A. Revcolevschi, Europhys. Lett., **62**, 540 (2003).
[5] E.-O. Giere, A. Brahimi, H. J. Deiseroth, and D. Reinen, J. Solid State Chem. **131**, 263 (1997).
[6] A. Nakua, H. Yun, J. N. Reimers, J. E. Greedan, and C. V. Stager, J. Solid State Chem. **91**, 105 (1991).
[7] M. Yamaguchi, T. Furuta, and M. Ishikawa, J. of Phys. Soc. of Jpn. **65**, 9, 2998 (1996)
[8] M. Kato, A. Hatazaki, K. Yoshimura, and K. Kosuge, Physica B **281-282**, 663 (2000)
[9] M. Kato, K. Kajimoto, K. Yoshimura, K. Kosuge, M. Nishi, and K. Kakurai, J. Phys. Soc. Jpn. 71, 187 (2002).
[10] A. V. Prokofiev, F. Ritter, W. Assmus, B. J. Gibson, and R. K. Kremer, J. Crystal Growth **247**, 457 (2003).
[11] M. Heinrich, H.-A. Krug von Nidda, A. Krimmel, A. Loidl, R. M. Eremina, A. D. Ineev, B. I. Kochelaev, A. V. Prokofiev, and W. Assmus, Phys. Rev. B **67**, 224418 (2003).

[12] B. J. Gibson, R. K. Kremer, A. V. Prokofiev, W. Assmus, and B. Ouladdiaf, J. Magn. Magn. Mat. **272**, 927 (2004).
[13] E. Wheeler, Ph.D Thesis, Somerville College, (University of Oxford, 2007).
[14] A. Rebello, M. G. Smith, J. J. Neumeier, B. D. White, and Yi-Kuo Yu, Phys. Rev. B **87**, 224427 (2013).
[15] D. Kasinathan, K. Koepernik, and H. Rosner, Phys. Rev. Lett. **100**, 237202 (2008).
[16] A. B. Christian, S. H. Masunaga, A. T. Schye, A. Rebello, and J. J. Neumeier, unpublished.
[17] B. D. Cullity, *Elements of X-ray Diffraction* (Addison-Wesley, 2001), 3rd Ed.
[18] A. Bystrom, B. Hok, and B. Mason, Arkiv. Kemi. Mineral. Geol. **15B**, No.4 (1941).
[19] R. Berman, *Thermal Conduction in Solids*, (Clarendon press, Oxford, 1976)
[20] J. des Cloizeaux and J. J. Pearson, Phys. Rev. **128**, 2131 (1962); L. D. Faddeev and L. A. Takhtajan, Phys. Lett. **85** A, 375 (1981).
[21] M. Hofmann, T. Lorenz, G. S. Uhrig, H. Kierspel, O. Zabara, A. Freimuth, H. Kageyama, and Y. Ueda, Phys. Rev. Lett. **87**, 047202 (2001).
[22] H. Winkelmann, E. Gamper, B. Buchner, M. Braden, A. Revcolevschi, and G. Dhalenne, Phys. Rev. B **51**, 12884 (1995).
[23] K. Berggold, J. Baier, D. Meier, J. A. Mydosh, T. Lorenz, J. Hemberger, A. Balbashov, N. Aliouane, and D. N. Argyriou, Phys. Rev. B **76**, 094418 (2007).
[24] J. G. Traylor, H. G. Smith, R. M. Nicklow, and M. K. Wilkinson, Phys. Rev. B **3**, 3457 (1971).
[25] Neelmani and G. S. Verma, Phys. Rev. B **6**, 3509 (1972).
[26] F. W. Sheard and G. A. Toombs, Solid state Commun. **12**, 713 (1973).
[27] W. N. Wybourne, B. J. Kiff, D. N. Bachelder, D. Greig, and M. Sahota, J. Phys. C **18**, 309 (1985).
[28] N. Hlubek, P. Ribeiro, R. Saint-Martin, A. Revcolevschi, G. Roth, G. Behr, B. Büchner, and C. Hess, Phys. Rev. B **81**, 020405(R) (2010).
[29] A. Mohan, N. Sekhar Beesetty, N. Hlubek, R. Saint-Martin, A. Revcolevschi, B. Büchner, and C. Hess, Phys. Rev. B **89**, 104302 (2014).